Artificial Intelligence in Agriculture 15 (2025) 564–572

Contents lists available at ScienceDirect

Artificial Intelligence in Agriculture

journal homepage: http://www.keaipublishing.com/en/journals/artificial-intelligence-in-agriculture/

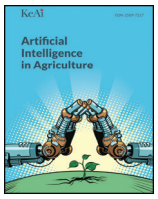

Research Paper

Unveiling the drivers contributing to global wheat yield shocks through quantile regression

Srishti Vishwakarma [a,b,*], Xin Zhang [a,*], Vyacheslav Lyubchich [c]

[a] Appalachian Laboratory, University of Maryland Center for Environmental Science, 301 Braddock Road, Frostburg, MD 21532, USA
[b] Computational Sciences and Engineering Division, Oak Ridge National Laboratory, 1 Bethel Valley Road, Oak Ridge, TN 37830, USA
[c] Chesapeake Biological Laboratory, University of Maryland Center for Environmental Science, 146 Williams Street, Solomons, MD 20688, USA

ARTICLE INFO

Article history:
Received 6 October 2024
Received in revised form 15 March 2025
Accepted 17 March 2025
Available online 22 March 2025

Keywords:
Linear quantile regression
Machine learning
Quantile random forest
Wheat yield shock

ABSTRACT

Sudden reductions in crop yield (i.e., yield shocks) severely disrupt the food supply, intensify food insecurity, depress farmers' welfare, and worsen a country's economic conditions. Here, we study the spatiotemporal patterns of wheat yield shocks, quantified by the lower quantiles of yield fluctuations, in 86 countries over 30 years. Furthermore, we assess the relationships between shocks and their key ecological and socioeconomic drivers using quantile regression based on statistical (linear quantile mixed model) and machine learning (quantile random forest) models. Using a panel dataset that captures spatiotemporal patterns of yield shocks and possible drivers in 86 countries, we find that the severity of yield shocks has been increasing globally since 1997. Moreover, our cross-validation exercise shows that quantile random forest outperforms the linear quantile regression model. Despite this performance difference, both models consistently reveal that the severity of shocks is associated with higher weather stress, nitrogen fertilizer application rate, and gross domestic product (GDP) per capita (a typical indicator for economic and technological advancement in a country). While the unexpected negative association between more severe wheat yield shocks and higher fertilizer application rate and GDP per capita does not imply a direct causal effect, they indicate that the advancement in wheat production has been primarily on achieving higher yields and less on lowering the possibility and magnitude of sharp yield reductions. Hence, in the context of growing extreme weather stress, there is a critical need to enhance the technology and management practices that mitigate yield shocks to improve the resilience of the world food systems.

1. Introduction

To meet rising food demand and ensure food security, increasing crop yield over the long term has been the focus of agricultural production (Ray et al., 2013). However, large year-to-year fluctuations in crop yield pose a significant threat to global food security. These fluctuations, if not within manageable limits, can trigger a cascade of effects on global food systems (Heslin et al., 2020). In particular, large and abrupt reductions in yield compared to its average level can result in shortages of crop products, reduced farmers' income, increased volatility of commodity markets, disrupted resilience of food supply, and a surge in food prices (Chen and Villoria, 2019; Davis et al., 2021; Tigchelaar et al., 2018). Such a situation is concerning for countries that are unable to absorb the shocks due to low economic and biophysical capacity, particularly those countries that rely on a handful of export countries. As the production of a major commodity concentrates in a few regionally specialized countries, simultaneous failure of production may become more likely, due to rising future vulnerabilities in the face of changing climatic conditions and extreme weather (Heslin et al., 2020; Mehrabi and Ramankutty, 2019; Tigchelaar et al., 2018). There is a need to understand the historical patterns of severe yield shocks to reduce crop production volatility caused by them.

While many studies have characterized spatiotemporal variations in crop yield, few have focused on yield shocks. The yield variability is primarily measured using statistical dispersion indicators such as the coefficient of variation (CV) and standard deviation (SD) (SI Appendix, Section S1). Implemented at multiple spatial scales (regional to global), these indicators include both positive and negative deviations of crop yield from its average. However, large negative deviations have a disproportionately higher adverse impact on farmers' revenues and amplify production-related risks. These negative deviations in yield are most felt by the world's poor, who spend 50–70 % of their income on

* Corresponding author.
E-mail addresses: vishwakarmas@ornl.gov (S. Vishwakarma), xin.zhang@umces.edu (X. Zhang).

https://doi.org/10.1016/j.aiia.2025.03.004

food (von Braun, 2008). Hence, this study addresses the critical global food security challenge by conducting an in-depth investigation on the spatiotemporal patterns of negative shocks and their drivers.

Among the limited number of studies on yield shocks, most define the yield shocks in a relative scale using the lower percentile of normalized yield anomalies (*Yield residuals*/*Expected yield*) (Cernay et al., 2015; Schauberger et al., 2018; Zhu et al., 2021). Although the normalization reduces dimension dependency and allows for cross-region comparison, it conceals the actual magnitude of shock, which is critical for food security. The size of a shock is required to assess the time and resources needed to recover from shocks while maintaining a country's food supply (Cottrell et al., 2019; Gephart et al., 2017). Therefore, in this study, we define yield shocks as lower quantiles of yield anomalies.

Although several studies have investigated potential drivers for yield shocks, many fall short in considering both ecological and socioeconomic drivers and quantifying their effects. Crop production is extremely sensitive to environmental conditions, especially climate and extreme weather (Gomez et al., 2021; Mueller et al., 2012; Ray et al., 2013; Tittonell et al., 2008; Zhu et al., 2021), but yield variability is also affected by other factors (Tigchelaar et al., 2018). A qualitative global shock assessment conducted by Cottrell et al. (2019) showed that about half of the crop sector shocks occurred due to climate and weather events, while the rest happened due to mismanagement, economic factors, geopolitical events, policy change, and other unknown factors. This demonstrates that, in addition to extreme weather and climate, it is critical to consider other drivers of yield shocks. In the thorough investigation by Cottrell et al. (2019), the drivers' assessment was qualitative, and their effects remained unquantified. Quantification of these effects is required to assess the shock risk in various countries and inform actions to reduce shocks. In this study, we quantitatively evaluated these shock-driver relationships.

We address the above research gaps with a focused data analysis by combining statistical and machine learning methods, applying them to extensive datasets on agricultural production, weather, and socioeconomic development, and extracting data-driven conclusions and recommendations. Using wheat as an example, we characterize yield shocks for countries around the world during 1979–2014 with the lower quantiles, such as 1 %, 5 %, and 10 %, of the yield fluctuations (see Section 2.1.5 for the definition of the yield fluctuations). Wheat is chosen because it is one of the staple crops that is grown, consumed, and traded globally (Asseng et al., 2015; Khater et al., 2023; Ray et al., 2015; Vishwakarma et al., 2022). Our quantile regression models investigate the relationship of both environmental (e.g., extreme weather stress) and socioeconomic (e.g., gross domestic product (GDP) per capita) drivers with the yield shocks. These types of models have rarely been implemented to yield shocks in particular. The quantile regression approach enables us to concentrate on the lower quantiles of crop yield anomalies (i.e., negative shocks) and assess their relationships with various drivers (Arshad et al., 2018; Barnwal and Kotani, 2013; Evenson and Mwabu, 2002; Gyamerah et al., 2019; Makowski et al., 2007; Nyamekye et al., 2016; Ricker-Gilbert and Jayne, 2012). This global study advances previous research on quantifying yield variability, shocks, and their drivers, and discusses the implications for food security.

2. Materials and methods

2.1. Data sources

This study examined the relationship between yield shocks and their drivers using panel data for 86 countries from 1979 to 2014. We derived the crop yield shocks from wheat yield (kg N ha^{-1} yr^{-1}) representing nitrogen (N) in the harvested crop from the Global Database of Nitrogen Budget in Crop Production (Zhang et al., 2015). The wheat yield is expressed in kg N ha^{-1} yr^{-1}, considering the protein provision per hectare of wheat plantation. This yield variable is a multiplication of the yield level and N content of crop wheat. Therefore, the spatial and temporal pattern of this yield variable is the same as that of yield measured by kg ha^{-1} yr^{-1} (SI Appendix, Section S3). The major drivers included extreme weather stress, GDP per capita, percentage value of agriculture in GDP (namely, agricultural GDP), N fertilizer application, and percentage area irrigated. Table 1 shows the data sources and spatiotemporal resolutions of the drivers. We also listed the hypothesized relationships of drivers with shocks and underlying mechanisms in SI Appendix, Table S1. The analysis was carried out for countries with at least ten years of wheat yield records. Furthermore, we eliminated those country and year combinations with missing data in either of the collected datasets. Countries that split or merged during the study period were analyzed as a single region (e.g., the Former Soviet Union).

Both climatic and non-climatic factors were examined as drivers of yield shocks. For the climate variables, we chose extreme weather stress as it has been shown in the past to adversely impact crop yield and food security. Under the category of non-climatic drivers, we considered four factors: N fertilization, area equipped for irrigation, per capita GDP, and percentage value of agriculture in GDP. While numerous other non-climatic factors can result in shocks, these variables were selected because of their strong relationship to country-level crop yields, high data quality, and low collinearity among them (SI Appendix, Fig. S7 and Table S3). We discussed the uncertainty and limitations of the unconsidered variables in the discussion section of this paper.

2.1.1. Extreme weather stress

To evaluate the extreme weather stress during the growing period of a crop, we developed a range of crop-specific extreme weather indices (Vishwakarma et al., 2022). These weather indices have been used to quantify the weather conditions that are outside the optimal crop growing conditions (Lyubchich et al., 2019; Zhu et al., 2015). The indices were derived in a five-step process. First, daily temperature and

Table 1
Data types and sources of variables used in the analysis.

Data	Data source	Spatial scale	Temporal scale
Weather			
Maximum temperature	ECMWF (Berrisford et al., 2011)	0.75°	1979–2014
Minimum temperature			
Total daily precipitation			
Crop presence			
Harvested area (ha)	Monfreda et al. (2008)	5 arcmin	2000
Crop calendar	Sacks et al. (2010)	0.5°	1–365 (day of year)
Wheat-specific nitrogen fertilization (kg N ha^{-1} yr^{-1})	Zhang et al. (2015)	86 countries	1979–2014
Wheat-specific nitrogen yield (kg N ha^{-1} yr^{-1})	Zhang et al. (2015)	86 countries	1979–2014
Area equipped with irrigation (1000 ha)	FAOSTAT (2018)	86 countries	1979–2014
Cropland area (1000 ha)	FAOSTAT (2018)	86 countries	1979–2014
GDP per capita (constant US$2010)	World Bank (2018)	86 countries	1979–2014
Agriculture, forestry, and fishing, value added (% of GDP)	World Bank (2018)	86 countries	1979–2014

precipitation data within the wheat growing season (based on the crop calendar map, Sacks et al. (2010)) were used to calculate 17 weather indices (SI Appendix, Table S5) for each grid cell and each year from 1979 to 2014. Second, using the gridded harvested area as weights, we aggregated each of the 17 weather indices to a national scale. Third, to reduce the dimensionality and avoid collinearity of the weather indices (SI Appendix, Fig. S21), we applied principal component analysis (PCA). With the heuristic elbow method, we selected the first two principal components (PCs) that represented heat and water, and cold weather stresses in a country (SI Appendix, Figs. S22-S23). Fourth, within each PC, we selected the dominant weather indices using the elbow method (SI Appendix, Fig. S23). The first PC is dominated by all cold stress related weather indices (i.e., Day growing degree low, DGDL, and Night growing degree low, NGDL). The second PC generally represents heat and water stress as it comprises the heat (i.e., Day growing degree high, DGDH) and drought (i.e, Precipitation low, PREL) indices (SI Appendix, Fig. S23). Finally, we calculated the extreme weather stress for each selected PC as a linear combination of the selected weather indices, weighted by the estimated contribution of the weather indices in that PC. We hypothesized that higher severity of shocks corresponds to higher weather stress in a country (SI Appendix, Table S1). We performed analyses for both spring wheat and winter wheat. Here we presented the results based on spring wheat, but the results for winter wheat are in SI Appendix, Section S11.

2.1.2. Gross domestic product (GDP) and agricultural GDP

The GDP per capita (constant US$2010) indicates the level of a country's economic development and technological advancement. The GDP per capita involves the investment in fertilizers, management practices, and machinery (Furman et al., 2002; Najafi et al., 2018). We included GDP per capita as one of the potential drivers in the analysis because we consider technological improvement to be one of the critical factors to reduce yield shocks. Furthermore, we considered the percentage share of the agricultural sector in total GDP, namely agricultural GDP, which indicates the contribution of agriculture to the economy of a country by producing goods and generating labor and capital. We hypothesized that higher GDP per capita and agricultural GDP correspond to smaller yield shocks and higher crop yields.

2.1.3. Nitrogen fertilizer application

Fertilizer is a regularly used input in the field by farmers to boost crop yield, influence grain protein concentration, and achieve yield stability. We hypothesized that higher N fertilizer application results in lower yield shocks and higher yields. N fertilizer application (kg N ha^{-1} yr^{-1}), obtained from Zhang et al. (2015), is the N fertilizer used on cropland at the country level.

2.1.4. Irrigated area

The establishment of irrigated facilities in a region tends to reduce the impact of climate variation on yield and, thus, the severity of shocks (Najafi et al., 2018). The fraction of cropland area equipped with irrigation was used in this study to quantify the role of irrigation in alleviating yield shocks. The percentage irrigated area (PIA) (Eq. 1) is the ratio of the land area equipped with irrigation (AEI) and the cropland area (CA):

$$PIA_{co,yr} = \frac{AEI_{co,yr}}{CA_{co,yr}} \tag{1}$$

where AEI includes the "areas equipped for full control irrigation, equipped lowland areas, and areas equipped for spate irrigation" (Portmann et al., 2010). The subscripts *co* and *yr* represent the country and year, respectively. The selection of AEI in this study is due to its high data quality and coverage of majority of countries compared to other country-level datasets representing irrigated area (e.g., wheat-specific irrigated area from AQUASTAT(FAO, 2018)).

2.1.5. Quantifying yield shocks

To quantify yield shocks, we chose lower quantiles (i.e., 1 %, 5 %, and 10 %) of yield fluctuations, which have been used to investigate extreme yield losses (Cernay et al., 2015; Schauberger et al., 2018; Zhu et al., 2021). The choice of quantiles was motivated by the impact of large abrupt yield declines and their consequent effects on food security. More specifically, in this study, a two-step approach was adopted to quantify yield shocks. First, we detrended each country's wheat yield time series using a locally weighted regression approach (Cleveland, 1979; Hastie et al., 2009) (see detailed steps in Vishwakarma et al. (2022) and SI Appendix, Section S3). We calculated the yield fluctuations as the difference between wheat yield and expected yield value. Our analysis focuses on the actual yield drop instead of the relative yield drop as it reflects the actual magnitude of the production gap required to fulfill the typical wheat demand in the supply chain, and it has a more direct effect on food security and consumer prices. In quantile regression models, these yield fluctuations were used as the response variable. Second, the lower quantiles of the fluctuations were calculated to quantify yield shocks per country and sub-period. We visualized these lower quantiles to describe the spatial and temporal patterns of the shocks (SI Appendix, Section S4). Since the yield fluctuations are defined as deviations from the local time mean (not from some fixed value), all deviations that adversely impact yields are negative numbers. Particularly, the lower quantiles of the fluctuations are negative; and more negative numbers imply more severe shocks. In addition to testing the actual yield fluctuations, we performed a sensitivity test using relative yield drops (SI Appendix, Table S2 and Fig. S6). Following these definitions of shocks, the hypothesized relationships of shocks with drivers are in SI Appendix, Table S1.

2.2. Modeling the effects of drivers on yield shocks

2.2.1. Linear quantile mixed model

The linear quantile mixed model (LQMM) was chosen to investigate the relationship between yield shocks and drivers because of its popularity in food security and agricultural studies, as well as its ease of regressing drivers on quantiles (Asante et al., 2021; D'Souza and Jolliffe, 2014; Kingwell and Xayavong, 2017; Penafiel et al., 2019; Tadesse et al., 2014). It is based on the parametric quantile regression approach, which is an extension of linear regression to analyze the conditional distribution of the response. In addition to the existing features of quantile regression, LQMM provides a flexible framework to include random intercepts and random slopes (Eq. 2). In this study, only random intercept was used at the level of the country:

$$Y_{[p]ct} = \alpha + \beta_i X_{ict} + \gamma_c + \epsilon_{ct} \tag{2}$$

where $Y_{[p]}$ represents is the p^{th} quantile of yield fluctuations, covariates X_i include heat and water stress, cold stress, N fertilization, per capita GDP, percentage value of agricultural GDP, and percentage irrigated area ($i = 1, \ldots, 6$), α and β are fixed intercept and slopes, γ is random intercept, $c = 1, \ldots, C$; C is the number of countries, ϵ is random error, and t represents the year. We used the R package lqmm (Geraci, 2014) to fit LQMMs. For selecting significant covariates in LQMM, stepwise regression was used with a forward selection approach.

This study employs a tree-based model (random forest), which is another form of additive models, instead of spline-based methods to approximate nonlinear relationships (Hastie et al., 2009). The parametric linear model (2) can be extended to a nonlinear case by replacing (some of) the coefficients β with nonparametric smooth functions $f(X)$. These functions provide local scatterplot smoothing by using linear or nonlinear building blocks such as the splines in generalized additive models (GAMs) and multivariate adaptive regression splines (MARS) (Hastie et al., 2009). Spline-based estimates are gaining popularity in the analysis of weather patterns (Lobell et al., 2011; Wongsai et al., 2017), crop yields (Bucheli et al., 2022; Lobell et al., 2014), and food

security (Hanspach et al., 2017; Na et al., 2022) due to their ability to accommodate the nonlinearity and nonmonotonicity of individual relationships.

2.2.2. Quantile random forest

Quantile random forest (QRF), a machine learning method, was adopted as a complementary nonparametric approach to validate the results of the LQMM analysis. Unlike LQMM, the QRF assesses nonlinear relationships between the shocks and their drivers. The R packages grf (Athey et al., 2019), ranger (Wright et al., 2017), and MML (Lyubchich, 2021) were used to fit the models and display partial dependence plots. To assess the statistical significance of the covariates in QRF, we used the 95 % simultaneous confidence intervals (SCIs) for the proportions of times each covariate was selected for making a split in the QRF trees. Covariates for which the lower end of the SCI was above zero were considered statistically significant. Furthermore, we assessed and ranked the importance of the covariates based on the proportions that were used for calculating SCI.

2.2.3. Assessing model performance

The model performance was evaluated in a cross-validation study. The cross-validation was repeated 100 times, with 70 % of the panel data randomly selected for training and the remaining 30 % for testing the models. The performance of each model was evaluated using the quantile-weighted errors (Eq. 3) (Haupt et al., 2011):

$$ATWE(p) = \frac{1}{n_p}\sum_{i=1}^{n_p}\rho_p(y_i - \hat{g}_i(p)) \quad (3)$$

where n_p is the number of observations, y_i is the observed values, $\hat{g}_i(\upsilon)$ represents the predicted quantiles, p is the probability for calculating quantiles (e.g., we used $p = 0.01$, 0.05, and 0.10), and ρ_p is the quantile loss function (Eq. 4):

$$\rho_p(u) = (p - I_{u<0})u, \quad (4)$$

where $I_{u<0}$ is the indicator function taking on the value of 1 when the inequality $u < 0$ is true and the value of 0 otherwise, and u is the input value of the quantile loss function.

A higher value of ATWE indicates a higher error, while a lower value shows a low error.

3. Results

3.1. Historical trends of crop yield variation

Although wheat yield has increased globally since 1979 (Fig. 1c), the variation of wheat yield has either increased or stagnated, and yield shocks have become more intense. The two indicators, SD and CV, typically used for measuring yield variability, show slightly different global trends: the distribution of SDs shifts to the right during the 9-year periods, suggesting increased variability (Fig. 1a); the shift in the distribution of CVs is less apparent and some countries have even shown a reduction in CV (Fig. 1b). Nevertheless, the lower quantiles of detrended yields indicate that negative shocks have intensified, as evidenced from the leftward shifts of the density curves (Figs. 1d-f). To further validate relationships observed in the density plots, we examined pairwise relationships between the yield shock indicators and the year using linear regression (SI Appendix, Table S8).

The general pattern of SD and CV observed globally still holds for most countries with only a few exceptions (SI Appendix, Figs. S1-S5). Both SD and CV of yield increase in European and African countries. In these two regions, a few countries, including Namibia, Mali, Chad, Niger, Sweden, France, and the Netherlands, have consistently experienced higher variability compared to other countries, particularly after 1988 (SI Appendix, Figs. S1 and S2). The same set of countries also faced large negative shocks (i.e., very low 1 % quantile) from 1997 to 2014 (SI Appendix, Fig. S3). The findings for these countries align with other studies assessing yield variability, demonstrating higher yield variations in European and African regions (Ben-Ari and Makowski, 2014). In western Europe, around 31–51 % yield variations are explained by climate variations (Ray et al., 2015). While climate variability could be one of the dominant factors impacting wheat yield variations, the remaining variations can be attributed to a complex interplay between management practices, regional characteristics, and geopolitical factors (Cottrell et al., 2019).

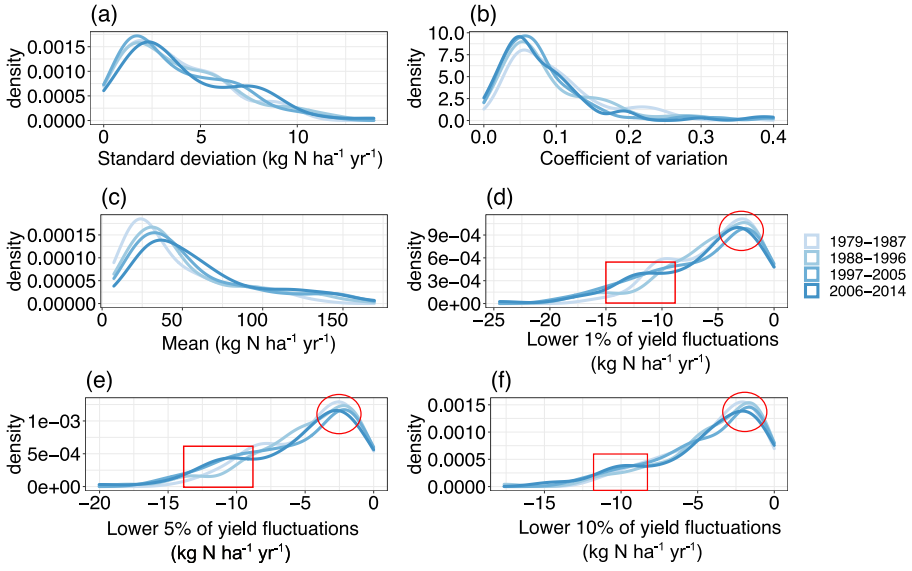

Fig. 1. Shifts in the distribution of yield and its variability over time, quantified with different indicators (panels a-f). The x-axes show the values of the indicator in kg N ha^{-1} yr^{-1} except for the coefficient of variation that is dimensionless, while the y-axes show the distribution densities estimated using Gaussian kernel and plotted using R package ggplot2 function geom_density(). Darker colored lines correspond to distributions for more recent sub-periods. The red circle demonstrates the declines in density (i.e., shocks of −5 to 0 kg N ha^{-1} yr^{-1} become less common) in the recent years, while red rectangles show heavier left tails (i.e., increase in yield shocks) in more recent sub-periods.

Table 2
Estimated coefficients of the linear quantile mixed models (LQMMs) for 1979–2014 for the three lower quantiles. Standard errors of the coefficients are in parentheses.

Response	Driver	Coefficient
Yield shock level (1 % quantile)	Heat and water stress	-1.86×10^{-3} (3.35×10^{-4})
	GDP per capita	-3.41×10^{-4} (4.22×10^{-5})
Yield shock level (5 % quantile)	Heat and water stress	-8.24×10^{-4} (1.18×10^{-4})
	Cold stress	-4.94×10^{-4} (1.83×10^{-4})
	GDP per capita	-2.34×10^{-4} (1.76×10^{-5})
Yield shock level (10 % quantile)	Heat and water stress	-5.42×10^{-4} (7.57×10^{-5})
	Cold stress	-3.68×10^{-4} (1.57×10^{-4})
	GDP per capita	-1.74×10^{-4} (2.19×10^{-5})

Note: see Method section for details related to the selection of drivers in the models.

3.2. Relationship between yield shocks and potential drivers

The results from both the quantile random forest (QRF) and linear quantile mixed model (LQMM) show that higher extreme weather stress corresponds to more severe yield shocks for all three selected shock levels (i.e., quantiles 1 %, 5 %, and 10 %; Table 2 and Fig. 2a-b). This finding is consistent with the hypothesized relationships (SI Appendix, Table S1). Besides linear relationships estimated with LQMM, the QRF, which is used as a complementary approach to LQMM, captures nonlinearities between shocks and extreme weather stress. The variables that indicate extreme weather stress conditions (e.g., heat and water stress, and cold stress) in this study are unitless, because they are derived using a dimensionality reduction technique, applied to a set of variables quantifying the number of days crops face extreme weather stress conditions within the growing period (see Method section for more information). Further exploring the partial dependence plots from QRF (Fig. 2a), we find more prominent negative relationships with the yield shocks when heat and water stress is in the range 6000–10,000, than when heat and water stress is below 6000. The majority of shocks in this range are seen in the Middle East and North Africa. The severity of shocks also increases with the increase in cold stress, especially when cold stress approaches the threshold of 2000 (Fig. 2b) but stagnates after that. The sudden drop in yield due to higher cold stress is typical for Eurasian countries such as Denmark, Hungary, and Norway. The shown pairwise relationships may not fully represent all the complexity of random forest models and interaction effects captured with consecutive tree splits. At all levels of quantiles, we found strong interaction of the heat and water stress with other variables (Molnar et al., 2022) (see SI Appendix, Section S12).

The per capita GDP is associated with severe yield shocks in both the QRF and LQMM. Further investigation of the data-driven relationship from QRF (Fig. 2d) confirms that countries with lower per capita GDP face less severe shocks compared to higher per capita GDP. The shock levels in countries with per capita GDP less than US$25,000 do not vary much, but become intense (i.e., more negative by about 4 kg N ha^{-1}-yr^{-1}) between US$25,000–50,000 of GDP per capita. Within this GDP range, some countries also show a slight alleviation in shocks level (for example, the USA in 2006–2007, Canada in 2012, and Sweden in 2004, when their per capita GDP was in the range of US $47,000–50,000). Overall, higher GDP corresponds to more severe

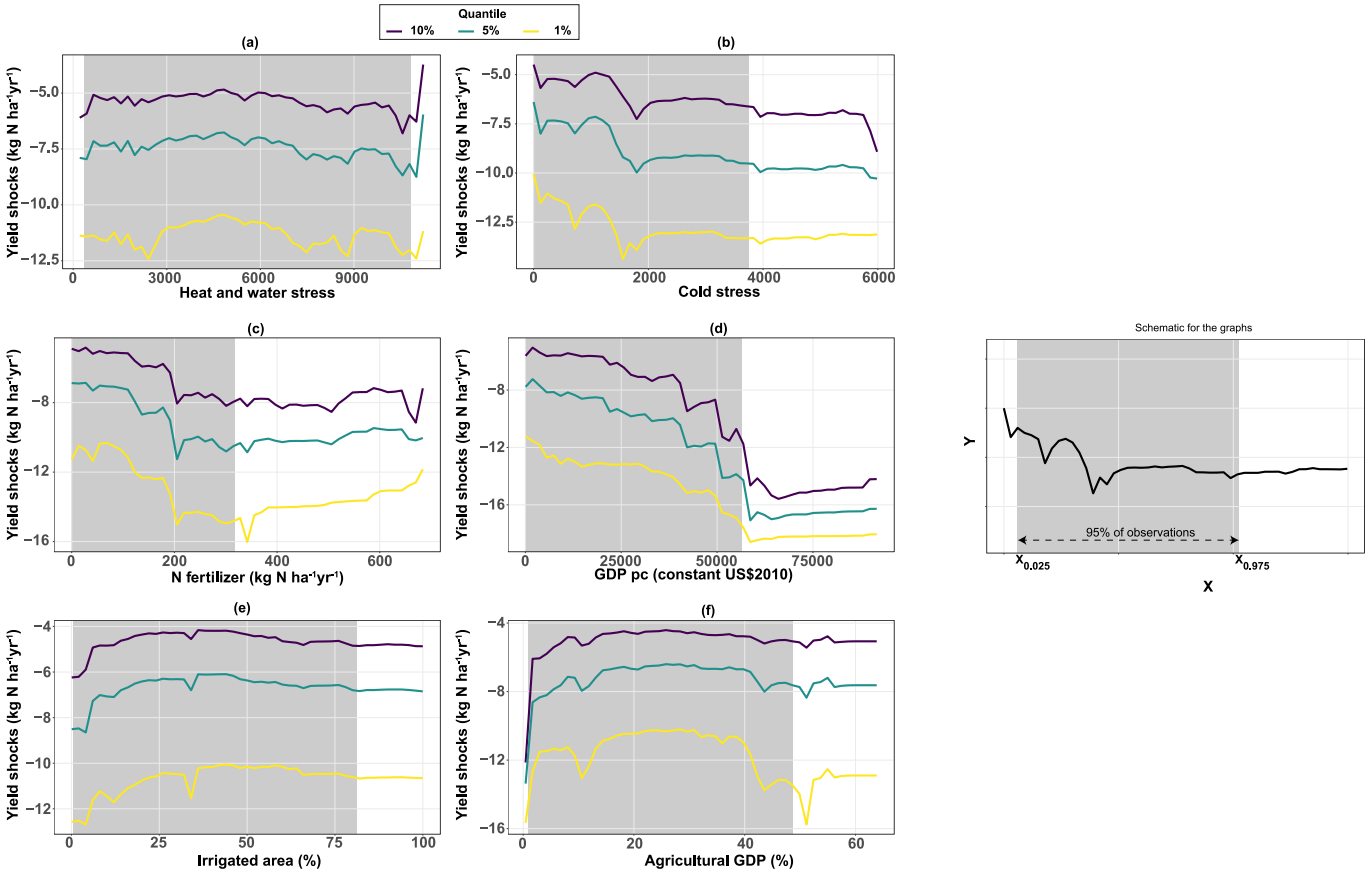

Fig. 2. Partial dependence plots resulting from quantile random forest for the three shock levels in 1979–2014. The shock levels are defined as three lower quantiles (1 %, 5 %, and 10 %) of yield fluctuations. The y-axis indicates average shock levels, while the x-axes show the drivers. The gray-shaded area spans between the 2.5 % and 97.5 % quantiles of covariate on the x-axis (i.e., covers the central 95 % of the cases). The schematic here demonstrates these partial dependence plots. The extreme weather stress variables (e.g., heat and water stress, and cold stress) are unitless as derived from the principal component analysis (see Method section for more information).

shocks, which refutes the proposed hypothesis that countries with higher GDP per capita tend to have better crop management and more resources and technologies available, resulting in less intense shocks (see the mechanism of impact in SI Appendix, Table S1).

In contrast to per capita GDP, increase in the percentage of agriculture's contribution to GDP (namely, agricultural GDP) corresponds to an overall decrease in severity of yield shocks. The shocks at all quantiles reduce by about 2 kg N ha^{-1} yr^{-1} with the increase in agriculture's contribution to GDP (Fig. 2f), except for a few extreme cases. Those exceptions show a sudden drop in shock (1 % quantile) between 40 and 50 % of agricultural GDP, mostly due to Chad and Niger in Sub-Saharan Africa. Among the few countries with agricultural GDP higher than 50 % (e.g., Nigeria), the 1 % and 5 %-quantile shocks show an extreme loss in yield.

Similar to per capita GDP, higher N fertilization also corresponds to severe shocks. The majority of countries' N fertilizer application rates range from 0 to 300 kg N ha^{-1} yr^{-1} (i.e., the gray-shaded area in Fig. 2c). According to the QRF model, the severity of yield shocks increases across all quantiles in that range of N fertilization. After a sudden increase in severity around 200 kg N ha^{-1} yr^{-1} of N fertilization, the change in severity of shocks slows down between 200 and 300 kg N ha^{-1} yr^{-1}. The countries falling in this range of N fertilization and shock levels include Bulgaria, Norway, Sweden, and the UK. Only a few countries have the application rates greater than 300 kg N ha^{-1} yr^{-1}. Among those countries, Ireland and the Netherlands are the primary locations for the large shocks at the 1 % quantile level.

The irrigated area exhibits a nonlinear relationship with yield shocks. For countries with an irrigated area of less than 25 %, an increase in irrigated area is accompanied by a reduction in the severity of shocks. In contrast, for countries that heavily rely on irrigation (e.g., where more than 50 % of cropland area is irrigated), higher irrigated area is associated with more severe shocks. Furthermore, in water-stressed countries such as Egypt and Iraq, where up to 100 % of cropland area is irrigated, shock severity levels off.

3.3. Different importance of drivers

Among all tested drivers for yield shocks, the three most important ones are heat and water stress, N fertilizer, and agricultural GDP. While these drivers remain the top three across all quantile levels tested in this study, their QRF-derived rankings differ across the models (SI Appendix, Fig. S8). In the QRF for 1 %-quantile shocks, heat and water stress (the most important) is followed by N fertilizer and agricultural GDP. At the 5 % shock level, N fertilizer ranks first, and heat and water stress ranks second. At the 10 % quantile, heat and water stress ranks first, followed by agricultural GDP and N fertilizer. Cold stress is the least important factor of all the considered shock quantiles, with the percentage irrigated area ranking second last. This ranking highlights the most important factors that can predict the severity of shocks.

3.4. Model performance

In the cross-validation study, we find that the QRF outperforms the LQMM in predicting shocks (Table 3). A lower average quantile-weighted absolute error (ATWE) indicates better performance of the model in estimating the desired quantile. The ATWE uses asymmetric penalties depending on the quantile, hence the values should be compared only for the same quantile (within each row of Table 3, not across the rows). This cross-validation study demonstrates the better ability of QRF to model quantiles by capturing the nonlinear relationships between shocks and drivers that cannot be modeled in the linear statistical model. Furthermore, in cross-validation, LQMM does not show statistical significance for the majority of drivers except for heat and water stress, cold stress, and GDP per capita. In the QRF model, however, all of the considered drivers are significant.

Table 3
Average quantile-weighted absolute error (ATWE, kg N ha^{-1} yr^{-1}) obtained from QRF and LQMM for three quantiles from 100 cross-validation runs.

Response	LQMM	QRF
Shock level (1 % quantile)	0.21	0.16
Shock level (5 % quantile)	0.57	0.52
Shock level (10 % quantile)	0.87	0.83

Note: QRF: quantile random forest; LQMM: linear quantile mixed model.

4. Discussion

4.1. Increasing severity of yield shocks and variations in yield

Many indicators have been used to quantify the year-to-year yield variation, but these indicators show different pictures. In this study, we considered three indicators, namely CV, SD, and lower quantiles (1 %, 5 %, and 10 %) of yield anomalies. Although less apparent, the CV decreases for some countries over time, indicating a decrease in variation of wheat yield. In contrast, SD and lower quantiles suggest an increase in variation and intensity of shocks, respectively.

Among these indicators, CV and SD use both the positive and negative fluctuations in the crop yield to assess the variation in wheat yield. The different historical trends of yield variability depicted by CV and SD are mainly caused by the increasing average yield. Overall, the assessment of SD emphasizes the yield variation in the absolute term, while CV emphasizes the yield variation in a relative term as it is normalized by the average yield level for the country during a certain period (Schauberger et al., 2018; Stuch et al., 2020).

In contrast to these two indicators, lower quantiles quantify the negative shocks in the crop yield. The negative shocks demonstrate the reduction in crop yield and the subsequent severe impact on the two critical dimensions of food security (i.e., food availability and food stability). In particular, we chose the lower quantiles (1 %, 5 %, and 10 %) of yield anomalies as indicators of shocks because they show extreme drops in crop yield that threaten food security. Our results show that in many countries the severity of shocks increased, and this could be of concern for reaching potential food supply targets by 2050 when the population is expected to rise by 9 billion (United Nations, 2019). Our analysis, based on the lower quantiles, will assist in the formulation of agricultural system policies for climate adaptation and mitigation to strengthen food security in many regions.

The variable patterns revealed by different indicators for yield variations highlight the importance of selecting indicators based on the scope of the study and the emphasis on food security. SD and CV can be used to quantify the overall historical variations of crop yield. However, indicators such as lower quantiles that emphasize large yield reductions (i.e., shocks) may assist in developing strategies to avoid potential shocks and mitigate their impact to maintain food supply and ensure food security.

4.2. The need to address yield shocks besides achieving higher yield

Although the relationship between shocks and extreme weather stress is consistent with studies that reported the sensitivity of crops to weather stress during the growing stage of crop (Arshad et al., 2018; Ben-Ari et al., 2018; Cottrell et al., 2019; Farooq et al., 2011; Gomez et al., 2021; Mondal et al., 2013), the association of shocks with the GDP and N fertilization observed from the RF partial dependence plots is unexpected. The partial dependence plots reveal nonlinear (thresholded) relationships between the yield shock and the two climatic stresses, which may correspond to a certain climatic region. For example, there is an apparent negative relationship when the heat and water stress is in the range of 6000–10,000, compared to when it is below 6000. This indicates that yield shocks tend to be more sensitive to heat and water stress when it is high. The LQMM results confirm

generally negative associations between the shocks and the weather stresses, although disregard the nonlinearity of these relationships. Both LQMM and RF show negative associations of shocks with GDP, and RF suggests a negative association between shocks and N fertilization during the research period 1979–2014.

After normalizing yield fluctuations by the average yield, the findings were generally consistent except for some of the relationships with N fertilization and GDP per capita (SI Appendix, Fig. S6). The LQMM shows a consistent negative relationship of GDP per capita with yield shocks (SI Appendix, Table S2, and Table 2), but the RF partial dependence plots provide more details on the nonlinearities. Thus, the partial dependence plots in SI Appendix Fig. S6d show the shocks become less severe when GDP rises to about US$7000, but shocks become more pronounced (more negative) for GDP higher than US$50,000. Analysis of relative yield shocks revealed that higher fertilization rates were associated with less severe relative shocks (i.e., fertilization of up to 100 kg N ha^{-1} yr^{-1} helped to reduce relative yield shocks, but higher fertilization rates did not result in further improvements, see Fig. S6c). These findings indicate that the unexpected relationships between fertilization rate, GDP, and more severe shocks may be associated with the higher average yield level enabled by increased fertilization but not matched with management practices that mitigate other disturbance to yield.

This study focuses on the actual size of shocks, which is crucial for food security. To further investigate these relationships, we classified countries based on their income levels (SI Appendix, Section S8). High-income countries have more resources to enhance yield (for example, N inputs and irrigation). Even with such resources, these countries are subject to severe shocks (although not necessarily severe relative shocks), demonstrating that advances in agricultural production technology and management approaches are primarily focused on achieving higher yields rather than reducing the severity of yield fluctuations (Bacsi and Hollósy, 2019; Najafi et al., 2018).

Contrary to per capita GDP, the severity of shocks either reduces or stays the same with the increase in the percentage share of the agriculture sector in GDP for majority of countries. Except for high-income nations, agriculture accounts for a sizable portion of GDP. A substantial contribution of agriculture to GDP demonstrates the importance of agriculture in the economy, especially in developing countries (Kim et al., 2019). Despite the importance of agricultural GDP in developing countries, heavy reliance of a country on agriculture makes it vulnerable to yield shocks as seen in the results. This potentially could result in a less stable economy and a difficult situation for future food security.

The unexpected results with GDP and N fertilization suggest the urgent need to alleviate yield shocks which have been often overlooked in the pursuit of higher yield. It is critical to guide the utilization of resources (e.g., fertilizer, labor, energy, irrigation, and land), investment in technology and management practices, and credit expansion initiatives from a focus on yield enhancement to reducing the severity of yield shocks and their consequential impacts on food security. Other adaptation strategies include investing in climate-smart agriculture (Lipper et al., 2014), diversifying production and supply to avoid overreliance on a few crops for production and consumption (Gomez et al., 2021; Renard and Tilman, 2019), and planting heat-tolerant crop varieties (Yadav et al., 2018). These adaptations can minimize negative repercussions that occur due to shocks (i.e., unemployment, migration, and conflicts) (Buhaug et al., 2015; Gephart et al., 2017) beyond the farm level.

4.3. Limitations and future research

Besides the six drivers tested in our modeling analysis, other factors may contribute to yield shocks. In addition to the six drivers, we examined a range of socioeconomic and ecological drivers, such as warfare and fertilizer prices. We checked the data quality and possible collinearity of those drivers (SI Appendix, Section S6). We find that data are available for various socioeconomic drivers globally, but many countries lack high-quality long-term data (SI Appendix, Table S3). For example, fertilizer price has a monumental influence on yield shocks due to its role in a farmer's decision to purchase fertilizer, but many developing countries have either zero-inflated data or missing values. Similar data constraints are observed when accounting for other variables such as agricultural machinery, refugees, and warfare. Other socioeconomic variables are available but are collinear with the variables already included in our models. For example, employment in agriculture was not used in the models because it strongly correlates with agriculture's contribution to GDP, which is a covariate used in this study (SI Appendix, Section S6). Water stress conditions play a crucial role in crop growth. Therefore, indicators for water stress (e.g., precipitation high (PREH) and precipitation low (PREL)) are among the 17 weather indices examined in this study (SI Appendix, Table S5). Many of these weather indices (e.g., NGDL and DGDL) have collinearity issues that need to be addressed before using the variables in a model (SI Appendix, Section S10). Therefore, we used a matrix of weather indices and reduced it to the top PCs and variables within. We named the first principal component (i.e., PC1) "cold stress" because it mostly consists of cold stress related weather indices (e.g., NGDL and DGDL), and the second principal component (i.e., PC2) is named "heat and water stress" due to the dominance of heat (i.e., DGDH) and water (i.e., PREL) stress related weather indices (SI Appendix, Fig. S23). The present methodology employed for developing new covariates to represent extreme weather stress conditions does not highlight precipitation as a dominant factor, forming a separate PC (SI Appendix, Fig. S23). Future research will focus on enhancing the existing approach to specifically investigate the individual impact of water stress, such as floods, on crop growth.

5. Conclusion

Our work shows that wheat yield shocks, measured by lower quantiles of yield fluctuations (i.e., 1 %, 5 %, and 10 %), have become more intense in the past decades. In comparison, standard deviation (SD) shows an increase in variation over time, while coefficient of variation (CV) shows a less apparent decrease in yield variation globally and some countries even show a reduction in CV. Quantile regression analysis shows that the severity of yield shocks increases with extreme weather stress, GDP per capita, and nitrogen fertilization, while it decreases with the percentage contribution of agriculture to GDP. The association of GDP per capita and fertilizer application with shocks suggests that efforts to improve cropping systems have prioritized increasing yields with less focus on mitigating intense yield shocks. Our findings highlight the importance of including historical assessments of shocks and their drivers when evaluating adaptive mechanisms at a national scale to improve the resilience of global food systems.

CRediT authorship contribution statement

Srishti Vishwakarma: Writing – review & editing, Writing – original draft, Visualization, Validation, Methodology, Investigation, Formal analysis, Data curation, Conceptualization. **Xin Zhang:** Writing – review & editing, Resources, Funding acquisition, Formal analysis, Conceptualization. **Vyacheslav Lyubchich:** Writing – review & editing, Visualization, Validation, Methodology, Investigation, Funding acquisition, Formal analysis, Conceptualization.

Declaration of competing interest

The authors declare no competing interest.

Acknowledgments

The funding support from the National Science Foundation CNS-1739823 is gratefully acknowledged. Xin Zhang would like to thank

the National Science Foundation (OISE-2330502, CBET-2047165, and CBET-2025826) and the Belmont Forum for support.

Appendix A. Supplementary data

Supplementary data to this article can be found online at https://doi.org/10.1016/j.aiia.2025.03.004.

References

Arshad, M., Amjath-Babu, T.S., Aravindakshan, S., Krupnik, T.J., Toussaint, V., Kächele, H., Müller, K., 2018. Climatic variability and thermal stress in Pakistan's rice and wheat systems: A stochastic frontier and quantile regression analysis of economic efficiency. Ecol. Indic. 89 (December 2017), 496–506. https://doi.org/10.1016/j.ecolind.2017.12.014.

Asante, P.A., Rozendaal, D.M.A., Rahn, E., Zuidema, P.A., Quaye, A.K., Asare, R., Läderach, P., Anten, N.P.R., 2021. Unravelling drivers of high variability of on-farm cocoa yields across environmental gradients in Ghana. Agr. Syst. 193, 103214. https://doi.org/10.1016/j.agsy.2021.103214.

Asseng, S., Ewert, F., Martre, P., Rötter, R.P., Lobell, D.B., Cammarano, D., Kimball, B.A., Ottman, M.J., Wall, G.W., White, J.W., Reynolds, M.P., Alderman, P.D., Prasad, P.V.V., Aggarwal, P.K., Anothai, J., Basso, B., Biernath, C., Challinor, A.J., De Sanctis, G., Zhu, Y., 2015. Rising temperatures reduce global wheat production. Nat. Clim. Change 5 (2), 143–147. https://doi.org/10.1038/nclimate2470.

Athey, S., Tibshirani, J., Wager, S., 2019. Generalized random forests. Ann. Stat. 47 (2), 1179–1203. https://doi.org/10.1214/18-AOS1709.

Bacsi, Z., Hollósy, Z., 2019. The yield stability index reloaded - the assessment of the stability of crop production technology. Agric. Conspec. Sci. 84 (4), 319–331.

Barnwal, P., Kotani, K., 2013. Climatic impacts across agricultural crop yield distributions: an application of quantile regression on rice crops in Andhra Pradesh, India. Ecol. Econ. 87, 95–109. https://doi.org/10.1016/j.ecolecon.2012.11.024.

Ben-Ari, T., Makowski, D., 2014. Decomposing global crop yield variability. Environ. Res. Lett. 9 (11). https://doi.org/10.1088/1748-9326/9/11/114011.

Ben-Ari, T., Boé, J., Ciais, P., Lecerf, R., Van der Velde, M., Makowski, D., 2018. Causes and implications of the unforeseen 2016 extreme yield loss in the breadbasket of France. Nat. Commun. 9 (1), 1627. https://doi.org/10.1038/s41467-018-04087-x.

Berrisford, P., Dee, D.P., Poli, P., Brugge, R., Fielding, M., Fuentes, M., Kållberg, P.W., Kobayashi, S., Uppala, S., Simmons, A., 2011. The ERA-interim archive version 2.0. *ERA Report Series* (ERA Report). ECMWF PP - Shinfield Park, Reading.

von Braun, J., 2008. The food crisis isn't over. Nature 456 (7223), 701. https://doi.org/10.1038/456701a.

Bucheli, J., Dalhaus, T., Finger, R., 2022. Temperature effects on crop yields in heat index insurance. Food Policy 107, 102214. https://doi.org/10.1016/j.foodpol.2021.102214.

Buhaug, H., Benjaminsen, T.A., Sjaastad, E., Magnus Theisen, O., 2015. Climate variability, food production shocks, and violent conflict in sub-Saharan Africa. Environ. Res. Lett. 10 (12), 125015. https://doi.org/10.1088/1748-9326/10/12/125015.

Cernay, C., Ben-Ari, T., Pelzer, E., Meynard, J.-M., Makowski, D., 2015. Estimating variability in grain legume yields across Europe and the Americas. Sci. Rep. 5 (1), 11171. https://doi.org/10.1038/srep11171.

Chen, B., Villoria, N.B., 2019. Climate shocks, food price stability and international trade: evidence from 76 maize markets in 27 net-importing countries. Environ. Res. Lett. 14 (1), 14007. https://doi.org/10.1088/1748-9326/aaf07f.

Cleveland, W.S., 1979. Robust locally weighted regression and smoothing scatterplots. J. Am. Stat. Assoc. https://doi.org/10.1080/01621459.1979.10481038.

Cottrell, R.S., Nash, K.L., Halpern, B.S., Remenyi, T.A., Corney, S.P., Fleming, A., Fulton, E.A., Hornborg, S., Johne, A., Watson, R.A., Blanchard, J.L., 2019. Food production shocks across land and sea. Nat. Sustainability 2 (2), 130–137. https://doi.org/10.1038/s41893-018-0210-1.

Davis, K.F., Downs, S., Gephart, J.A., 2021. Towards food supply chain resilience to environmental shocks. Nat. Food 2 (1), 54–65. https://doi.org/10.1038/s43016-020-00196-3.

D'Souza, A., Jolliffe, D., 2014. Food insecurity invulnerable populations: Copingwith foodprice shocks in Afghanistan. Am. J. Agric. Econ. 96 (3), 790–812. https://doi.org/10.1093/ajae/aat089.

Evenson, R.E., Mwabu, G., 2002. The effects of agricultural extension on farm yields in Kenya. Afr. Dev. Rev. 13, 1–23. https://doi.org/10.1111/1467-8268.00028.

FAO, 2018. AQUASTAT Database. AQUASTAT. http://www.fao.org/nr/water/aquastat/data/query/index.html?lang=en.

FAOSTAT, 2018. FAOSTAT: Statistical database. Statistical Database, FAOSTAT.

Farooq, M., Bramley, H., Palta, J.A., Siddique, K.H.M., 2011. Heat stress in wheat during reproductive and grain-filling phases. Crit. Rev. Plant Sci. 30 (6), 491–507. https://doi.org/10.1080/07352689.2011.615687.

Furman, J.L., Porter, M.E., Stern, S., 2002. The determinants of national innovative capacity. Res. Policy 31 (6), 899–933. https://doi.org/10.1016/S0048-7333(01)00152-4.

Gephart, J.A., Deutsch, L., Pace, M.L., Troell, M., Seekell, D.A., 2017. Shocks to fish production: identification, trends, and consequences. Glob. Environ. Chang. 42, 24–32. https://doi.org/10.1016/j.gloenvcha.2016.11.003.

Geraci, M., 2014. Linear quantile mixed models: the lqmm package for Laplace quantile regression. J. Stat. Softw. 57 (13), 1–29. https://doi.org/10.18637/jss.v057.i13.

Gomez, M., Mejia, A., Ruddell, B.L., Rushforth, R.R., 2021. Supply chain diversity buffers cities against food shocks Michael. Preprint 595 (July), 1–17. https://doi.org/10.1038/s41586-021-03621-0.

Gyamerah, S.A., Ngare, P., Ikpe, D., 2019. Crop yield probability density forecasting via quantile random forest and Epanechnikov Kernel function. https://doi.org/10.1016/j.ecolmodel.2014.01.030.

Hanspach, J., Abson, D.J., French Collier, N., Dorresteijn, I., Schultner, J., Fischer, J., 2017. From trade-offs to synergies in food security and biodiversity conservation. Front. Ecol. Environ. 15 (9), 489–494. https://doi.org/10.1002/fee.1632.

Hastie, T., Tibshirani, R., Friedman, J., 2009. The elements of statistical learning. Elements Stat. Learn. https://doi.org/10.1007/978-0-387-84858-7.

Haupt, H., Kagerer, K., Schnurbus, J., 2011. Cross-validating fit and predictive accuracy of nonlinear quantile regressions. J. Appl. Stat. 38 (12), 2939–2954. https://doi.org/10.1080/02664763.2011.573542.

Heslin, A., Puma, M.J., Marchand, P., Carr, J.A., Dell'Angelo, J., D'Odorico, P., Gephart, J.A., Kummu, M., Porkka, M., Rulli, M.C., Seekell, D.A., Suweis, S., Tavoni, A., 2020. Simulating the cascading effects of an extreme agricultural production shock: global implications of a contemporary US dust bowl event. Front. Sustain. Food Syst. 4 (March), 1–12. https://doi.org/10.3389/fsufs.2020.00026.

Khater, A., Fouda, O., El-Termezy, G., Abdel hamid, S., El-Tantawy, M., El-Beba, A., Sabry, H., & Okasha, M., 2023. Modification of the rice combine harvester for cutting and binding wheat crop. J. Agri. Food Res. 14, 100738. https://doi.org/10.1016/j.jafr.2023.100738.

Kim, W., Iizumi, T., Nishimori, M., 2019. Global patterns of crop production losses associated with droughts from 1983 to 2009. J. Appl. Meteorol. Climatol. 58 (6), 1233–1244. https://doi.org/10.1175/JAMC-D-18-0174.1.

Kingwell, R.S., Xayavong, V., 2017. How drought affects the financial characteristics of Australian farm businesses. Aust. J. Agric. Resour. Econ. 61 (3), 344–366. https://doi.org/10.1111/1467-8489.12195.

Lipper, L., Thornton, P., Campbell, B.M., Baedeker, T., Braimoh, A., Bwalya, M., Caron, P., Cattaneo, A., Garrity, D., Henry, K., Hottle, R., Jackson, L., Jarvis, A., Kossam, F., Mann, W., McCarthy, N., Meybeck, A., Neufeldt, H., Remington, T., Torquebiau, E.F., 2014. Climate-smart agriculture for food security. Nat. Clim. Change 4 (12), 1068–1072. https://doi.org/10.1038/nclimate2437.

Lobell, D.B., Bänziger, M., Magorokosho, C., Vivek, B., 2011. Nonlinear heat effects on African maize as evidenced by historical yield trials. Nat. Clim. Chang. 1 (1), 42–45. https://doi.org/10.1038/nclimate1043.

Lobell, D.B., Roberts, M.J., Schlenker, W., Braun, N., Little, B.B., Rejesus, R.M., Hammer, G.L., 2014. Greater sensitivity to drought accompanies maize yield increase in the U.S. Midwest. Science 344 (6183), 516–519. https://doi.org/10.1126/science.1251423.

Lyubchich, V., 2021. CRAN - package MML: Misc machine learning. Version 0.0.2.

Lyubchich, V., Newlands, N.K., Ghahari, A., Mahdi, T., Gel, Y.R., 2019. Insurance risk assessment in the face of climate change: integrating data science and statistics. WIREs Computat. Stat. 11 (4), e1462. https://doi.org/10.1002/wics.1462.

Makowski, D., Doré, T., Monod, H., 2007. A new method to analyse relationships between yield components with boundary lines. Agron. Sustain. Dev. 27 (2), 119–128. https://doi.org/10.1051/agro:2006029.

Mehrabi, Z., Ramankutty, N., 2019. Synchronized failure of global crop production. Nat. Ecol. Evol. 3 (5), 780–786. https://doi.org/10.1038/s41559-019-0862-x.

Molnar, C., König, G., Herbinger, J., Freiesleben, T., Dandl, S., Scholbeck, C.A., Casalicchio, G., Grosse-Wentrup, M., Bischl, B., 2022. General pitfalls of model-agnostic interpretation methods for machine learning models. In: Holzinger, A., Goebel, R., Fong, R., Moon, T., Müller, K.-R., Samek, W. (Eds.), xxAI - Beyond Explainable AI: International Workshop, Held in Conjunction with ICML 2020, July 18, 2020, Vienna, Austria, Revised and Extended Papers (pp. 39–68). Springer International Publishing https://doi.org/10.1007/978-3-031-04083-2_4.

Mondal, S., Singh, R.P., Crossa, J., Huerta-Espino, J., Sharma, I., Chatrath, R., Singh, G.P., Sohu, V.S., Mavi, G.S., Sukuru, V.S.P., Kalappanavar, I.K., Mishra, V.K., Hussain, M., Gautam, N.R., Uddin, J., Barma, N.C.D., Hakim, A., Joshi, A.K., 2013. Earliness in wheat: A key to adaptation under terminal and continual high temperature stress in South Asia. Field Crop Res. 151, 19–26. https://doi.org/10.1016/j.fcr.2013.06.015.

Monfreda, C., Ramankutty, N., Foley, J.A., 2008. Farming the planet: 2. Geographic distribution of crop areas, yields, physiological types, and net primary production in the year 2000. Global Biogeochem. Cycles 22 (1), 1–19. https://doi.org/10.1029/2007GB002947.

Mueller, N.D., Gerber, J.S., Johnston, M., Ray, D.K., Ramankutty, N., Foley, J.A., 2012. Closing yield gaps through nutrient and water management. Nature 490 (7419), 254–257. https://doi.org/10.1038/nature11420.

Na, M., Dou, N., Liao, Y., Rincon, S.J., Francis, L.A., Graham-Engeland, J.E., Murray-Kolb, L.E., Li, R., 2022. Daily food insecurity predicts lower positive and higher negative affect: an ecological momentary assessment study. Front. Nutr. 9.

Najafi, E., Devineni, N., Khanbilvardi, R.M., Kogan, F., 2018. Understanding the changes in global crop yields through changes in climate and technology. Earth's Future 6 (3), 410–427. https://doi.org/10.1002/2017EF000690.

Nyamekye, I., Services, G., E-mail, T., Fiankor, D.D., 2016. Effect of human capital on maize productivity in Ghana: a quantile regression approach. Int. J. Food Agric. Econ. 4 (2), 125–135. https://doi.org/10.22004/ag.econ.234914.

Penafiel, D., Cevallos-Valdiviezo, H., Espinel, R., Van Damme, P., 2019. Local traditional foods contribute to diversity and species richness of rural women's diet in Ecuador. Public Health Nutr. 22 (16), 2962–2971. https://doi.org/10.1017/S136898001900226X.

Portmann, F.T., Siebert, S., Döll, P., 2010. MIRCA2000-global monthly irrigated and rainfed crop areas around the year 2000: A new high-resolution data set for agricultural and hydrological modeling. Global Biogeochem. Cycles 24 (1). https://doi.org/10.1029/2008gb003435.

Ray, D.K., Mueller, N.D., West, P.C., Foley, J.A., 2013. Yield Trends Are Insufficient to Double Global Crop Production by 2050. 8(6). https://doi.org/10.1371/journal.pone.0066428.

Ray, D.K., Gerber, J.S., MacDonald, G.K., West, P.C., 2015. Climate variation explains a third of global crop yield variability. Nat. Commun. 6, 5989. https://doi.org/10.1038/ncomms6989.

Renard, D., Tilman, D., 2019. National food production stabilized by crop diversity. Nature https://doi.org/10.1038/s41586-019-1316-y.

Ricker-Gilbert, J., Jayne, T.S., 2012. Do fertilizer subsidies boost staple crop production and reduce poverty across the distribution of smallholders in Africa? Quantile regression results from Malawi. International Association of Agricultural Economists (IAAE) triennial conference, Foz Do Iguaçu, Brazil, 18-24 august, 2012 https://doi.org/10.22004/ag.econ.126742.

Sacks, W.J., Deryng, D., Foley, J.A., Ramankutty, N., 2010. Crop planting dates: an analysis of global patterns. Glob. Ecol. Biogeogr. 19 (5), 607–620. https://doi.org/10.1111/j.1466-8238.2010.00551.x.

Schauberger, B., Ben-Ari, T., Makowski, D., Kato, T., Kato, H., Ciais, P., 2018. Yield trends, variability and stagnation analysis of major crops in France over more than a century. Sci. Rep. 8 (1), 1–12. https://doi.org/10.1038/s41598-018-35351-1.

Stuch, B., Alcamo, J., Schaldach, R., 2020. Projected climate change impacts on mean and year-to-year variability of yield of key smallholder crops in sub-Saharan Africa. Clim. Dev. 0(0), 1–15. https://doi.org/10.1080/17565529.2020.1760771.

Tadesse, G., Algieri, B., Kalkuhl, M., von Braun, J., 2014. Drivers and triggers of international food price spikes and volatility. Food Policy 47, 117–128. https://doi.org/10.1016/j.foodpol.2013.08.014.

Tigchelaar, M., Battisti, D.S., Naylor, R.L., Ray, D.K., 2018. Future warming increases probability of globally synchronized maize production shocks. Proc. Natl. Acad. Sci. U. S. A. 115 (26), 6644–6649. https://doi.org/10.1073/pnas.1718031115.

Tittonell, P., Vanlauwe, B., Corbeels, M., Giller, K.E., 2008. Yield gaps, nutrient use efficiencies and response to fertilisers by maize across heterogeneous smallholder farms of western Kenya. Plant Soil 313 (1–2), 19–37. https://doi.org/10.1007/s11104-008-9676-3.

United Nations, 2019. World Population Prospects 2019: Data Booklet [PDF]. Date of Access: 12 December 2019, retrieved from: *https://population.un.org/wpp/Publications/Files/WPP2019_DataBooklet.pdf*.

Vishwakarma, S., Zhang, X., Lyubchich, V., 2022. Wheat trade tends to happen between countries with contrasting extreme weather stress and synchronous yield variation. Commun. Earth Environ. 3 (1), 261. https://doi.org/10.1038/s43247-022-00591-7.

Wongsai, N., Wongsai, S., Huete, A., 2017. Annual seasonality extraction using the cubic spline function and decadal trend in temporal daytime MODIS LST data. Remote Sens. (Basel) 9, 1254. https://doi.org/10.3390/rs9121254.

World Bank, 2018. World Development Indicators.

Wright, M.N., Wager, S., Probst, P., 2017. CRAN - package ranger: A fast implementation of random forests. Version 0.12.1.

Yadav, S., Redden, R., Hatfield, J., Ebert, A., Hunter, D., 2018. Food Security and Climate Change. https://doi.org/10.1002/9781119180661.

Zhang, X., Davidson, E.A., Mauzerall, D.L., Searchinger, T.D., Dumas, P., Shen, Y., 2015. Managing nitrogen for sustainable development. Nature 528 (7580), 51–59. https://doi.org/10.1038/nature15743.

Zhu, P., Abramoff, R., Makowski, D., Ciais, P., 2021. Uncovering the past and future climate drivers of wheat yield shocks in Europe with machine learning. Earth's Future 9 (5), 1–13. https://doi.org/10.1029/2020EF001815.

Zhu, W., Porth, L., Tan, K.S., 2015. A credibility-based yield forecasting model for crop reinsurance pricing and weather risk management. SSRN 1 (204), 1–36. https://doi.org/10.2139/ssrn.2663932.